

Impurity scattering and quantum confinement in giant magnetoresistance systems

Peter Zahn,¹ Jörg Binder,² and Ingrid Mertig¹

¹*Fachbereich Physik, Martin-Luther-Universität Halle-Wittenberg, D-06099 Halle, Germany*

²*Institut für Theoretische Physik, Technische Universität Dresden, D-01062 Dresden, Germany*

(Dated: April 14, 2004)

Ab initio calculations for the giant magnetoresistance (GMR) in Co/Cu, Fe/Cr, and Fe/Au multilayers are presented. The electronic structure of the multilayers and the scattering potentials of point defects therein are calculated self-consistently. Residual resistivities are obtained by solving the quasi-classical Boltzmann equation including the electronic structure of the layered system, the anisotropic scattering cross sections derived by a Green's function method and the vertex corrections. Furthermore, the influence of scattering centers at the interfaces and within the metallic layers is incorporated by averaging the scattering cross sections of different impurities at various sites. An excellent agreement of experimental and theoretical results concerning the general trend of GMR in Co/Cu systems depending on the type and the position of impurities is obtained. Due to the quantum confinement in magnetic multilayers GMR can be tailored as a function of the impurity position. In Co/Cu and Fe/Au systems impurities in the magnetic layer lead to high GMR values, whereas in Fe/Cr systems defects at the interfaces are most efficient to increase GMR.

PACS numbers: 73.63.-b, 75.70.Cn, 75.30.Et, 71.15.Mb

INTRODUCTION

A large number of experimental and theoretical investigations was initiated by the discovery of giant magnetoresistance (GMR) in magnetic multilayers [1, 2] to elucidate the microscopic origin of the phenomenon. Several authors have shown [3, 4] that GMR in magnetic multilayers is strongly influenced by changes in the electronic structure, especially the Fermi velocities, of the system in dependence on the relative magnetization alignment in adjacent layers. In realistic samples, however, spin-dependent scattering is considered to cause GMR. The effort to tailor GMR systems with high rates was accompanied by a variety of experiments [5, 6] and calculations [7, 8, 9] which investigated the influence of doping and impurities. Agreement was reached concerning the dominant role of interface scattering [5]. The results of Marrows et al. [6], however, demonstrated the strong dependence of GMR on the position of the impurities with respect to the interfaces and on the valence difference between impurity and host. The aim of this paper is to present ab initio calculations for the scattering cross sections and resulting GMR ratios in dependence on defect material and position for the standard systems of magnetoelectronics Co/Cu and Fe/Cr. In addition, the system Fe/Au was investigated because the system shows a high interface quality [10] and the structural properties should be closest in experiment and theory. The influence of defects on interlayer exchange coupling in Fe/Au was investigated earlier [11].

METHOD

All calculations are performed within the framework of density functional theory in local spin density approximation applying the Screened KKR (Korringa-Kohn-Rostoker) Green's function method [12]. We have chosen a multilayer geometry in the so-called first antiferromagnetic (AF) maximum of interlayer exchange coupling for the Co/Cu system consisting of 9 monolayers (ML) Co separated by 7 ML Cu, denoted as Co₉Cu₇. The structure of the superlattice was assumed to be an fcc lattice with a lattice constant of 6.76 a.u. grown in (001) direction. Each atomic plane is represented by one atom in the prolonged unit cell with 32 atoms. A similar configuration was chosen for Fe/Cr and a perfect bcc stacking in (001) direction with a lattice constant of 5.50 a.u. was assumed. This is somewhat larger than the lattice constant of Fe and Cr, but provides the correct magnetic order within the LDA and the atomic sphere approximation for the potentials [13]. The Fe/Cr system consists of 9 ML Fe and 9 ML Cr which possesses an AF ground state confirmed by calculation and experiment [10]. Structural relaxations at the interfaces were neglected. Despite of the AF order the Cr layer will be referred to as the non-magnetic layer in the system, to use the same notation as for the other system under consideration. We consider Fe/Au multilayers with the same structural data reported by the experiments [10] that is a structural bcc-fcc transition. The lattice constant for Fe is $a_{\text{bcc}} = 5.4163 \text{ a.u.}$; and for Au $a_{\text{fcc}} = \sqrt{2} a_{\text{bcc}}$. The thickness of 9 ML of the Au layer was chosen in accordance with the experimentally obtained interlayer exchange coupling strength which favors an antiparallel coupling for this Au thickness.

The self-consistent electronic structure of the ideal host, without any impurities, is described by the one-

particle Green's-function, whose structural part $G_{\mathbf{L}\mathbf{L}^0}^{nn^0}(\mathbf{E})$ is expanded into a site and angular-momentum basis [14].

The new aspect for superlattices is that we consider a lattice with a basis. The index n is now a shorthand notation for lattice vector \mathbf{R}_n and basis vector \mathbf{r}_i of the atoms in the unit cell. To simulate a substitutional point defect one atom in the lattice is replaced by another. The site index of the impurity position is denoted by \mathbf{r} .

The impurity Green's function $G_{\mathbf{L}\mathbf{L}^0}^{nn^0}(\mathbf{E})$ of the multilayer including an impurity atom at a defined position is obtained by the solution of an algebraic Dyson equation [14]

$$G_{\mathbf{L}\mathbf{L}^0}^{nn^0}(\mathbf{E}) = G_{\mathbf{L}\mathbf{L}^0}^{nn^0}(\mathbf{E}) + \sum_{\mathbf{n}^0\mathbf{L}^0} G_{\mathbf{L}\mathbf{L}^0}^{nn^0}(\mathbf{E}) t_{\mathbf{L}^0}^{n^0}(\mathbf{E}) G_{\mathbf{L}^0\mathbf{L}^0}^{n^0n^0}(\mathbf{E}) : \quad (1)$$

The n^0 -summation involves all sites in the vicinity of the site \mathbf{r} for which the differences of the single site t -matrices $t_{\mathbf{L}^0}^{n^0} = t_{\mathbf{L}^0}^{n^0} - t_{\mathbf{L}^0}^{n^0}$ of the multilayer with and without defect are significant. The single site t -matrices are derived from the angular-momentum dependent scattering phase shifts of the potentials in atomic sphere approximation (ASA). The differences $t_{\mathbf{L}^0}^{n^0}$ characterize the potential perturbation caused by the defect. In the calculations we take into account angular momenta $l_{\mathbf{m}ax} = 3$. We allow for potential perturbations up to the second atomic shell around the impurity atom. Charge multipoles up to $l_{\mathbf{m}ax} = 6$ are taken into account. Since the systems under consideration are magnetic all properties mentioned above depend also on spin quantum numbers $\sigma = \uparrow, \downarrow$ for majority and minority electrons, respectively.

Using the impurity Green function, the self-consistently calculated potential perturbation and the wave function coefficients of the superlattice Bloch states we derive the microscopic spin-conserving transition probability $P_{\mathbf{k}\mathbf{k}^0}$ for elastic, that is on-shell-scattering of a Bloch wave \mathbf{k} into a perturbed Bloch wave \mathbf{k}^0 . \mathbf{k} is now a shorthand notation for the wave vector \mathbf{k} and band index n , σ denotes the spin quantum number [15, 16]. The transition probability is given by Fermi's golden rule

$$P_{\mathbf{k}\mathbf{k}^0} = 2\pi \mathcal{N} \mathcal{T}_{\mathbf{k}\mathbf{k}^0}^2(\mathbf{E}_{\mathbf{k}} - \mathbf{E}_{\mathbf{k}^0}) : \quad (2)$$

The formalism is restricted to dilute alloys since we assume a linear dependence with the number of defects \mathcal{N} . Furthermore, spin-orbit coupling and the resulting spin-flip processes are neglected by the non-relativistic scheme.

The transition matrix elements $T_{\mathbf{k}\mathbf{k}^0}$ for the scattering of Bloch electrons by an impurity cluster embedded in an otherwise ideal translational invariant multilayer are given by [16, 17]

$$T_{\mathbf{k}\mathbf{k}^0} = \frac{1}{V} \sum_{\mathbf{L}\mathbf{L}^0\mathbf{n}\mathbf{n}^0} C_{\mathbf{L}}^n(\mathbf{k}; \sigma) T_{\mathbf{L}\mathbf{L}^0}^{nn^0} C_{\mathbf{L}^0}^{n^0}(\mathbf{k}^0; \sigma) : \quad (3)$$

$C_{\mathbf{L}}^n(\mathbf{k}; \sigma)$ are the expansion coefficients for the superlattice wave function in an angular momentum basis. V denotes the total crystal volume. Using spherical potentials (ASA) the matrix elements $T_{\mathbf{L}\mathbf{L}^0}^{nn^0}$ are derived from the structural Green's function matrix elements $G_{\mathbf{L}\mathbf{L}^0}^{nn^0}$ of the perturbed system and the potential perturbation $t_{\mathbf{L}^0}^{n^0}$ [17, 18, 19].

Summation over all final states leads to the spin and state dependent relaxation time

$$\frac{1}{\tau_{\mathbf{k}}(\sigma)} = \sum_{\mathbf{k}^0} P_{\mathbf{k}\mathbf{k}^0}(\sigma) \quad (4)$$

which depends on spin σ , Bloch state \mathbf{k} and impurity position \mathbf{r} in the superlattice. The \mathbf{k} and spin-dependence of the scattering rates is treated fully quantum-mechanically without adjustable parameter. The dependence on the effect position is involved by the implicit dependence of the impurity Green's function $G_{\mathbf{L}\mathbf{L}^0}^{nn^0}$ on the \mathbf{r} . Up to this point we consider a dilute alloy of impurity atoms all of them occupying a chosen site \mathbf{r} in the unit cell. That is, the alloying is restricted to certain atomic planes in the multilayer. These planes correspond to the impurity \mathbf{r} -layers experimentally investigated by Marrows and Hickey [6].

The conductivity is calculated by solving the quasi-classical Boltzmann equation [16]. Thus, the vector mean free paths are obtained by

$$\mathbf{l}_{\mathbf{k}}(\sigma) = \mathbf{l}_{\mathbf{k}}(\sigma) \mathbf{v}_{\mathbf{k}} + \sum_{\mathbf{k}^0} P_{\mathbf{k}\mathbf{k}^0}(\sigma) \mathbf{l}_{\mathbf{k}^0}(\sigma) : \quad (5)$$

This includes besides to the anisotropic relaxation times as the second term on the r.h.s the computational demanding scattering-in term (vertex corrections) which completes the description of impurity scattering [16, 20]. The band structure is included via Fermi velocities $\mathbf{v}_{\mathbf{k}}$ and the \mathbf{k}^0 summation over all states on the anisotropic Fermi surface. The impurity scattering enters via the relaxation times $\tau_{\mathbf{k}}(\sigma)$ and the microscopic transition probabilities $P_{\mathbf{k}\mathbf{k}^0}(\sigma)$. Eq. (5) is solved iteratively to determine the vector mean free path $\mathbf{l}_{\mathbf{k}}(\sigma)$ of an electron with spin σ in a state \mathbf{k} . To our knowledge, up to now the semi-classical calculations of the GMR have been mostly performed within relaxation time approximation only [8, 9, 21, 22, 23, 24], which neglects the scattering-in term. Zhang and Butler proposed a simplified method to include the vertex corrections by renormalization of the electron life times using an adjustable parameter [25]. The deviation of the relaxation time approximation in comparison with the solution including the vertex corrections are discussed in Fig. 2.

Based on the solution of Eq. (5) the spin-dependent conductivity tensor $\sigma_{\alpha\beta}(\sigma)$ is given by a Fermi surface integral [16]

$$\sigma_{\alpha\beta}(\sigma) = \frac{e^2}{V} \sum_{\mathbf{k}} (\mathbf{E}_{\mathbf{k}} - \mathbf{E}_{\mathbf{F}})_{\alpha} \mathbf{l}_{\mathbf{k}}(\sigma)_{\beta} \mathbf{v}_{\mathbf{k}} : \quad (6)$$

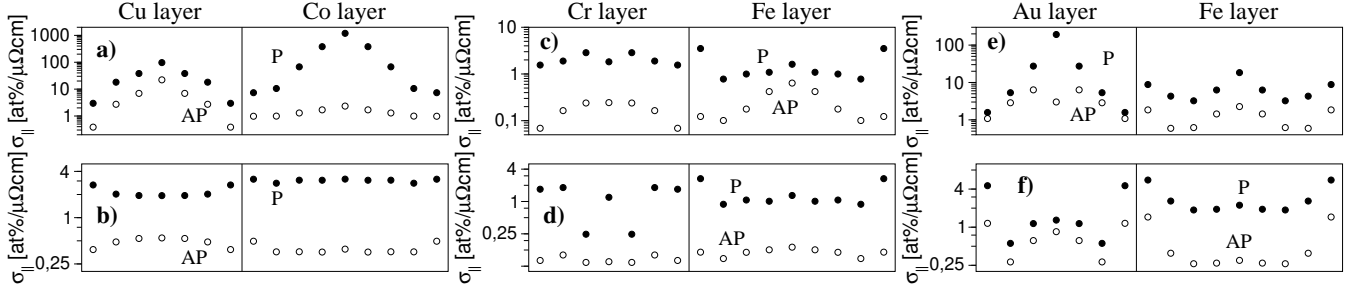


FIG. 1: Conductivity of $\text{Cu}_{99}\text{Cu}_{01}$, $\text{Fe}_{99}\text{Cr}_{01}$, and $\text{Fe}_{99}\text{Au}_{01}$ for P and AP alignment in dependence on the position of 'self' impurities, respectively; a,c,e) Assuming scattering at the inserted δ -layer only, b,d,f) assuming δ -layer scattering (50%) and interface scattering (50%)

With Mott's two current model [26] the total conductivity $\sigma_{\parallel} = \sigma_{\parallel}^{\uparrow} + \sigma_{\parallel}^{\downarrow}$ is obtained by spin summation. The CIP resistivity is obtained by the inverse of the CIP conductivity due to the diagonal structure of the conductivity tensor for the tetragonal systems under consideration

$$\rho_{\parallel} = \frac{1}{\sigma_{\parallel}^{\uparrow} + \sigma_{\parallel}^{\downarrow}} \quad (7)$$

To describe the existence of an overall distribution of impurities in the multilayer the transition probabilities of the different δ -layers have to be superimposed. Following this idea, layer-dependent relaxation times τ_k are added

$$\frac{1}{\tau_k} = \sum_{\mathbf{x}} \frac{x(\mathbf{x})}{\tau_k(\mathbf{x})}; \quad (8)$$

including weighting factors $x(\mathbf{x})$ that account for the relative concentration of defects at the corresponding positions \mathbf{x} in the unit cell.

The most driving aspect of magnetic multilayers is the drastic change of the conductivity as a function of the relative orientation of the magnetic layer moments, parallel (P) or anti-parallel (AP). The relative change defines the GMR ratio

$$\text{GMR}(\mathbf{x}) = \frac{\rho_{\parallel}^{\text{P}}(\mathbf{x})}{\rho_{\parallel}^{\text{AP}}(\mathbf{x})} - 1. \quad (9)$$

CONDUCTIVITY AND QUANTUM WELL STATES

We consider the multilayers described above and investigate the scattering properties of impurities of the nonmagnetic component in the magnetic layers and vice versa.

The analysis of the transport coefficients is focused on the current-in-plane (CIP) geometry. The total CIP-conductivities normalized to the defect concentration c caused by impurities of the magnetic material at different positions in the nonmagnetic layer and nonmagnetic

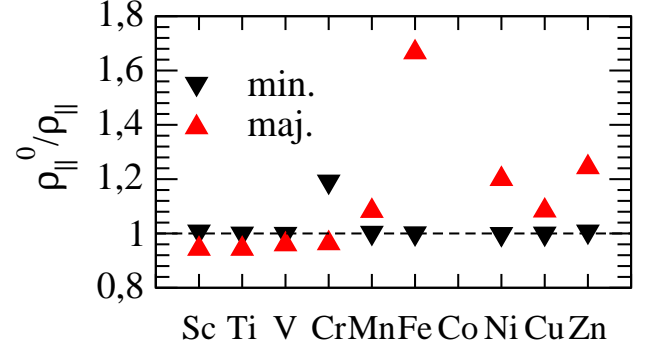


FIG. 2: Influence of vertex corrections: Dependence of the spin dependent resistivity for $\text{Cu}_{99}\text{Cu}_{01}$ multilayers on 3d impurities at the interface position of the magnetic layer ρ_{\parallel}^0 calculated including vertex corrections and ρ_{\parallel} without

defects in the magnetic layer are shown for all considered systems in Fig. 1a,c,e), respectively, for both configurations of the magnetization directions (P, AP). The conductivity differs by orders of magnitude as a function of impurity position (keep in mind the logarithmic scale). The largest values occur for impurity positions where the quantum confinement produces many Bloch states with low probability amplitude. The eigenstates show strong quantum confinement due to the superlattice potential. That is, the probability amplitude is modulated by the layered structure and can even tend to zero at particular sites of the supercell [8, 24]. The consideration of additional interface scattering in Fig. 1 b,d,f) will be discussed below.

The influence of vertex corrections is quantified in Fig. 2. For different defects at the Co interface position in Co/Cu the deviation of the resistivity ρ_{\parallel}^0 calculated including vertex corrections in Eq. (5) and without (ρ_{\parallel}) are shown for both spin bands. In the minority channel (upwards triangles) the deviations are of the order of few percent (except for Cr). In the majority channel the vertex corrections are large for defects where sp-scattering dominates. This is the case for impurities with a similar electronic structure like the host, at least for this spin

direction. For Sc, Ti, V, and Cr with an opposite magnetic moment with respect to Co and a dominating sd scattering the vertex corrections are small as for the minority spin direction. Summarizing, one can state, that the variations of the resistivity by incorporation of the vertex corrections in the solution of the Boltzmann equation are less than 20% and do not change the qualitative behaviour of GMR. The neglect of vertex corrections may change the results quantitatively, but the general trend is conserved.

To analyze the influence of the quantum confinement on the character of the eigenstates a classification of the eigenstates according to Ref. [8] was performed. The distribution of the probability amplitude in the different regions of the multilayer was analyzed and the states are labeled by the region with the highest averaged probability amplitude. The eigenstates are classified in 4 types and are labeled by quantum well states (QWS) in the magnetic layer C_M (Co, Fe), QWS in the nonmagnetic layer C_N (Cu, Cr, Au), interface states C_I , and extended states C_E which have a probability amplitude of approximately the same size in all regions. To emphasize the contribution of the different classes of eigenstates the total conductivity (Eq. (6)) was projected to the layers in the supercell according to Ref. [27]

$$\sigma_{\parallel}(r_i) = \frac{e^2}{V} \sum_{\mathbf{k}} (\mathbf{E}_{\mathbf{k}} - \mathbf{E}_F) \mathbf{v}_{\mathbf{k},\parallel} \mathbf{v}_{\mathbf{k},\parallel} \frac{1}{\tau_{\mathbf{k}}} \left| \sum_{\mathbf{r}_i} c_{\mathbf{k}}(\mathbf{r}_i) \right|^2 ; \quad (10)$$

with $c_{\mathbf{k}}(\mathbf{r}_i)$ the expansion coefficient of the Bloch eigenstate $(\mathbf{k}, \mathbf{r}_i)$ at the site \mathbf{r}_i in the supercell. The normalization of the Bloch state to the unit cell yields $\sum_{\mathbf{r}_i} |c_{\mathbf{k}}(\mathbf{r}_i)|^2 = 1$. In addition, the site dependent conductivity $\sigma_{\parallel}(r_i)$ was split into the contributions of the 4 typical classes of eigenstates which are shown in Fig. 3. It is evident, that a large contribution of the CIP conductivity is carried by the QWS in the magnetic and nonmagnetic layer. Especially, in the minority channel of the Co/Cu system and the majority channel of the Fe/Cr system the conductivity is dominated by contributions of the magnetic quantum well states. By considering only a few types of defects in the sample the conductivity is dominated by one spin direction in most cases. Assuming more types of defects and taking into account the effect of self averaging this tendency is reduced.

Due to the quantum size effects the relaxation times show a strong variation for the states at the Fermi level which determine the conductivity. All Bloch states with a nearly zero probability amplitude at the impurity site undergo a weak scattering and cause extremely large relaxation times. The state dependent relaxation times are distributed over several orders of magnitude, especially for defects inside the metallic layers (see Fig. 4). This is a new effect that does not occur in bulk systems. The panels show the relative amount of relaxation times $\tau_{\mathbf{k}}$ for the states at the Fermi level for the Co/Cu system (top

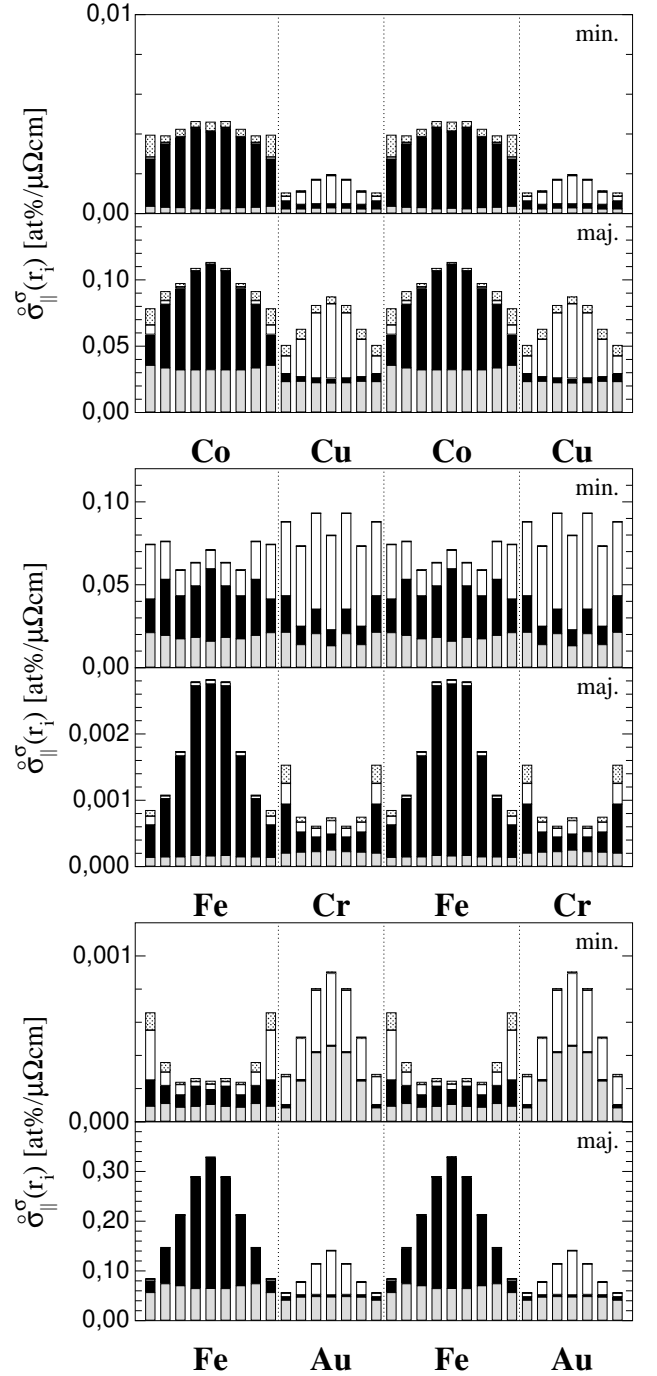


FIG. 3: Spin-dependent, layer-projected conductivity of Co_9Cu_7 , Fe_9Cr_7 , and Fe_9Au_7 for P alignment with interface defects, typical classes are marked by grey - extended, black - magnetic QWS (Co, Fe), white - nonmagnetic QWS (Cu, Cr, Au), and light grey interface states.

viewgraph) and the Fe/Cr system (bottom panel). The spin resolved histograms for Cu defects in bulk Co are given for comparison (topmost subpanel). The remaining subpanels represent relaxation times for Cu defects in the center of the Co layer and for Cu defects at the

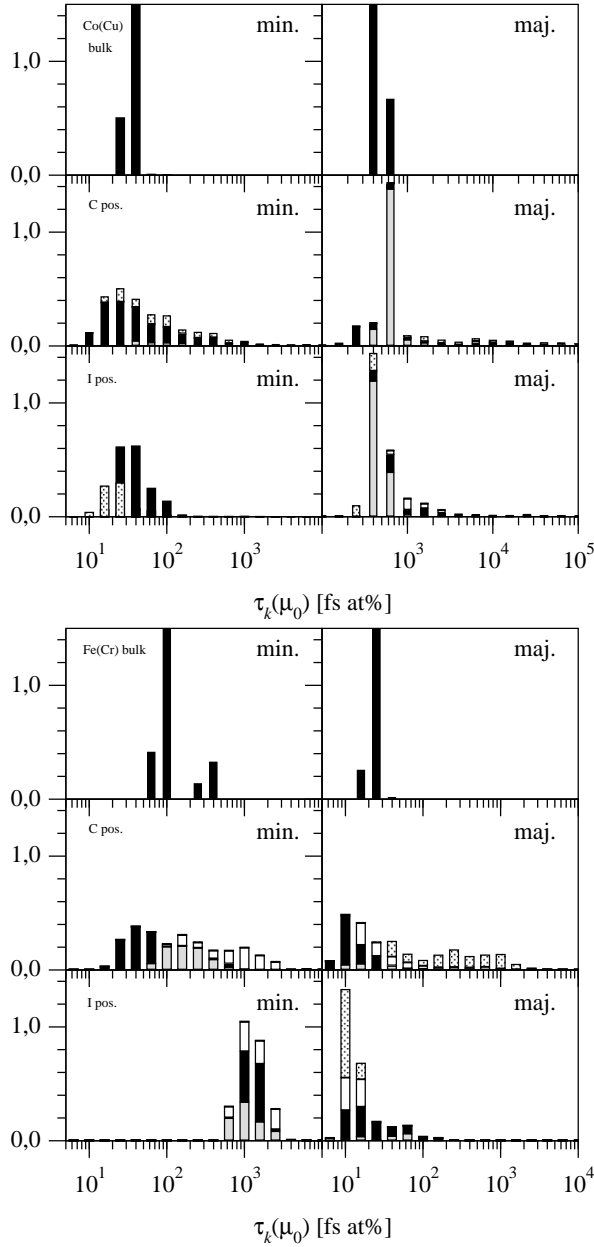


FIG. 4: histogram of spin-dependent, anisotropic relaxation times of $\text{Co}_{90}\text{Cu}_{10}$ (top panel), and $\text{Fe}_{90}\text{Cr}_{10}$ (bottom panel) for P alignment, defects in the magnetic layer at interface position (bottom), center position (middle), and defect in bulk (top), the contribution of typical classes are marked by grey - extended, black - Co/Fe, white - Cu/Cr/Au, and light grey - interface states

Co/Cu interface. The color of the bars labels the character of the eigenstates: extended multilayer states are shown in dark grey, QWS confined to the magnetic layer are shown in black. QWS confined to the nonmagnetic layer are given in white, and interface states are given by light grey bars. For defects inside the magnetic layer the maximum of the distribution coincides with that in the bulk material. In addition, a long tail for high values

occurs caused by states which have a small probability amplitude at the defect position, e.g. quantum well states in the nonmagnetic layer or interface states. This is best seen in the middle subpanel for Cr defects in the center of the Fe layer for the Fe/Cr multilayer. Quantum well states confined to the Fe layer have a large probability amplitude at the defect position and as a result smaller relaxation times than in the bulk system. Interface states with a tail penetrating the Fe layer are scattered on an intermediate level and Cr quantum well states with the lowest probability amplitude at the defect position are scattered weakly.

The states with large relaxation times although not numerous are highly conducting and nearly provoke a short circuit. This is the case for Co impurities in the Cu layer for the Co/Cu multilayer, compare Fig. 4, top panel, and for Fe defects in the Au layer for the Fe/Au system. This effect is mainly obtained for impurities in the center of the layers and is related to the fact that in-plane transport is mostly driven by quantum well states [8]. This peculiar behavior of conductivity is in agreement with the results of Blaas et al. [9] who found higher resistivities for Co/Cu multilayers with interdiffusion restricted to the interface layers than for alloying with Cu atoms in the Co layers.

For comparison with experiments we have to mention that the large absolute values would hardly be obtained experimentally since they correspond to idealized samples with perfectly flat interfaces and defects at well defined positions in the superlattice. As soon as we consider an overall distribution of defects in the multilayer the highly conducting channels are suppressed. The general trend, however, survives. This phenomenon of highly conducting electrons confined to one layer of a multilayer structure is called electron wave guide or channeling effect [24, 28] and was also experimentally verified [29].

Structural investigations of Co/Cu multilayers on an atomic scale [30, 31] gave evidence that most of the structural imperfections appear next to the interfaces. To investigate the influence of more than one type of scattering centers in one sample a simplified defect distribution was assumed. In addition to the specific δ -layer defects of the magnetic layer material in the nonmagnetic interface atomic layer and defects from the nonmagnetic material in the magnetic interface layer are considered to simulate an intermixed region at the interface. For the concentration weights $x(\delta)$ entering Eq. (8) we choose 25% for defects in both of the interface layer and 50% for defects in the δ -layer and the resulting conductivities are shown in Fig. 1(b),(d),(f), respectively. First, an overall reduction of the resistivities is obtained, caused by the distribution of defects at different positions and the resulting higher probability that also quantum well states are scattered at one or the other type of defect. According to Eq. (8) the defect with the highest scattering rate $1=\tau_k$ dominates the total relaxation time τ_k .

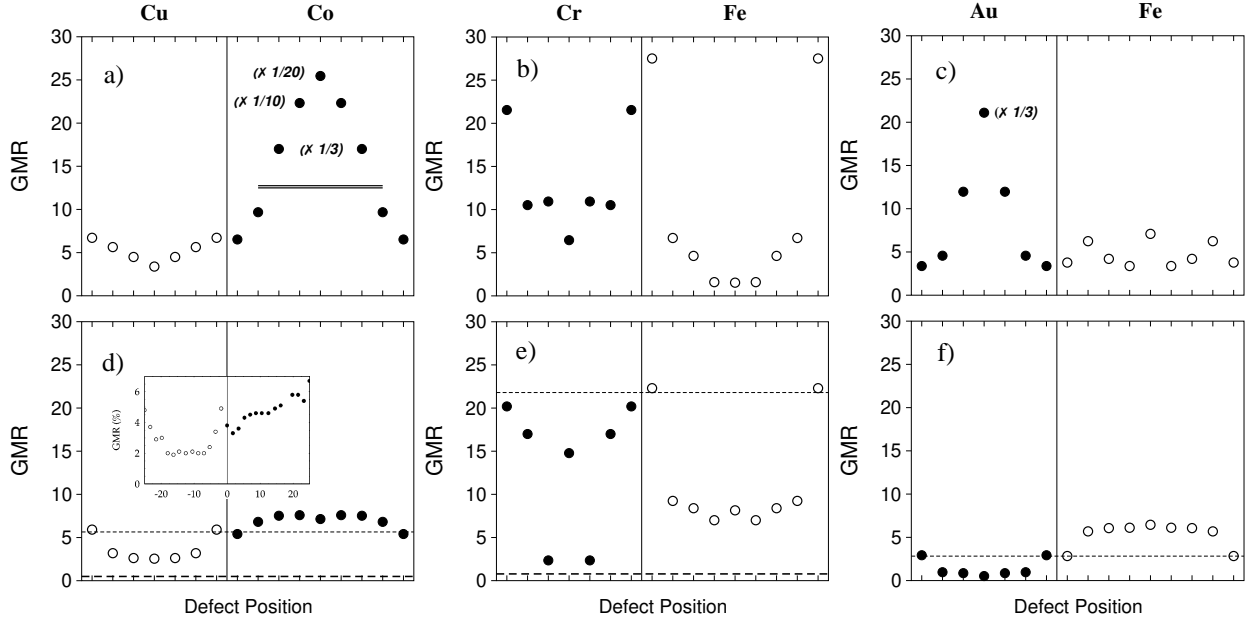


FIG. 5: Dependence of GMR in Cu/Co , Fe/Cr , and Fe/Au on the position of 'self' impurities. a-c) Assuming scattering at the inserted γ -layer only, d-f) assuming γ -layer scattering (50%) and interface scattering (50%). The thin dashed line marks the GMR ratio assuming interface impurities only, and the thick dashed line gives the GMR assuming isotropic relaxation times. the inset in panel (d) shows the experimental result from Ref. [6]

GIANT MAGNETORESISTANCE

The GMR ratios derived from the conductivities in Fig. 1 are shown in Fig. 5. Assuming scattering centers in the γ -layer only (Fig. 5 (a),(c),(e)) huge GMR ratios are obtained especially for Cu defects in the Co layer. Introducing additional interface scattering with a weight of 50% causes strongly reduced values (Fig. 5(b),(d),(f)). The thin dashed line in the lower panels of Fig. 5 is the GMR ratio caused by interface scattering. This value would correspond to the reference value in the experiments of Marrows and Hickey without γ -layer [6]. The thick dashed line in Fig. 5 gives the GMR value obtained with the assumption of a constant relaxation time without any spin or state dependence (intrinsic GMR). In comparison to this case of isotropic scattering the insertion of an additional γ -layer increases GMR, mostly at the interfaces.

Comparing the trend of GMR an excellent agreement with the experiment (inset in Fig. 5) is obtained for the Co/Cu system. To our knowledge, up to now similar experimental investigations of the GMR dependence on the defects position are not available for Fe/Cr multilayers. The importance of the interface scattering to obtain a large GMR effect in Fe/Cr was pointed out by several authors [32, 33, 34]. The weighting factors for the different scattering mechanisms are derived from the structural investigations by Davies et al. [32]. We choose 0.45 for Cr defects in the Fe interface atomic layers and 0.05 for Fe defects in the Cr interface layer. The contribution

from the γ -layer is fixed to 0.5 as in the case of the Co/Cu multilayer. The most striking feature in comparison to Co/Cu is the reduction of the GMR ratio by introducing Cr defects in the Fe layers as shown in Fig. 5(b) and e).

We still have to mention, that the calculated values are two orders of magnitude larger than the experimental ones. The reason is the restriction to substitutional point defects. In addition to these much more scattering mechanisms are active in real samples. Assuming self-averaging the results could be corrected towards the experimental ones by an additional spin- and state-independent relaxation time (thick dashed line in fig. 2d-f) [8].

In contrast to Ref. [35] the present results were obtained assuming the above described impurity distribution only and are focussed on the impurity scattering rates only. Another difference to the experimental setup in Ref. [36] is the considered geometry. The experimentally investigated samples have been Co/Cu/Co spin valves grown on a buffer layer and protected by a cap layer. As a consequence the GMR ratios are nearly symmetric as a function of the impurity position in the Cu layer but asymmetric for defects in the Co layer. The calculations are performed in supercell geometry which is reflected in the symmetry of the results with respect to the defect position in both layers, Cu and Co. A possible influence of superlattice effects in metallic multilayers was shown to be negligible [37].

Fig. 6 compiles the trend of GMR caused by 3d-, 4s- (left column) and 4d-, 5s-transition metal impurities

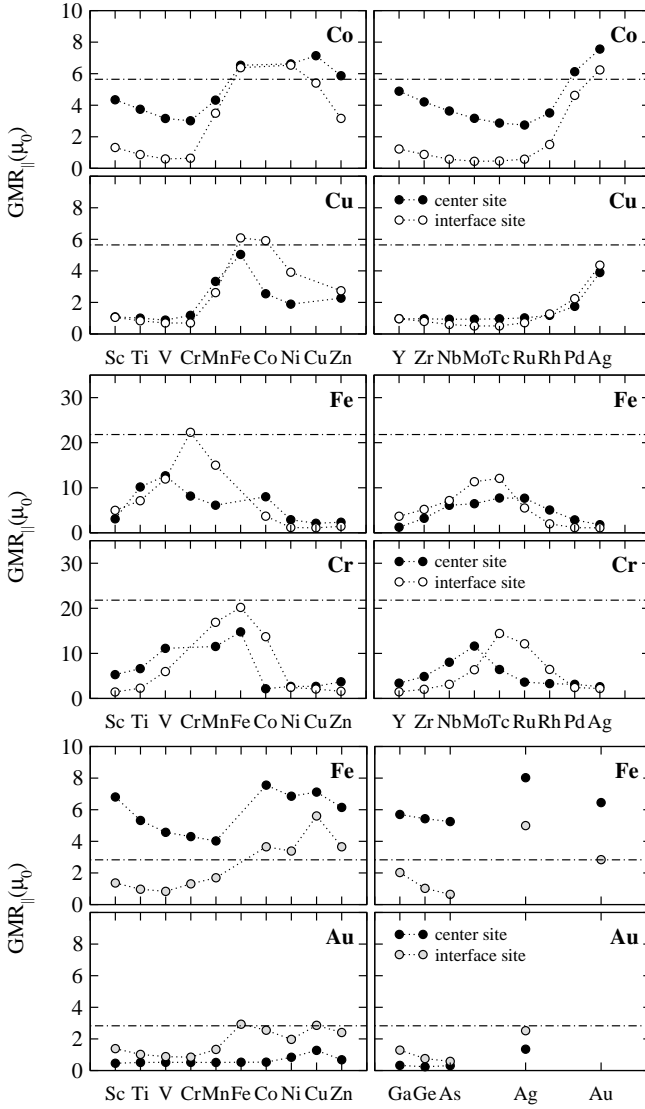


FIG. 6: Dependence of the GMR on the impurity δ -layer doped with different transition and sp-metals and the position in the in $C_{O_9}=C_{U_7}$ (top panel), $F_{O_9}=C_{U_7}$ (middle panel), and $F_{O_9}=A_{U_7}$ (lower panel); the label of each subpanel denotes the layer where the δ -layer is inserted; closed symbols: positions in the center, and open symbols mark the interface positions

(right column) as a function of position in the magnetic layer. The CIP-GMR ratios are given for the corresponding defects in the middle of the magnetic and nonmagnetic layer, respectively, marked by the closed symbols. The open symbols correspond to a position of the δ -layer at the interface. The horizontal dashed lines indicate the case of interface scattering only. This means we consider a δ -layer of the magnetic material in the nonmagnetic interface atomic layer and vice versa. The thick dashed lines give the results assuming a spin and state independent relaxation time.

In a previous work [8] we used a simplified model to describe the scattering. We assumed δ -peak like potential

perturbations characterized by a spin-dependent scattering strength τ . Comparing with these results one can state the following. The reader should note that the order of Co and Cu in Fig. 2 in ref. [8] is reversed in comparison to Fig. 5a) and d) of this work. The insertion of a δ -layer in the Co layer enhances the GMR in comparison to the undoped case in both models. The differences of the results are caused by the approximation used for the scattering strength. In this work the scattering potentials were determined self consistently also for a region around the defects. Evaluating Eq. (3) the Born series expansion of the scattering operator T in terms of the single site t -matrix and all multiple scattering contributions are included completely.

Comparing the influence of 3d defects at the interface with that caused by an ordered interface alloy [38] a similar trend for the GMR is obtained. One should compare Fig. 5 (left column) in ref. [38] and the GMR values for the position $x = 0$ of the δ -layer in Fig. 6. For the lighter 3d elements up to Mn the GMR is lowered with the interface alloy, whereas for heavier elements the GMR is maintained or even increased.

All the calculations are carried out for the limit of low defect concentration. That means the scattering at different defects is treated independently. For a typical concentration of 1% we obtain an imaginary part of the self energy of the order of 10^{-3} eV. This is small in comparison with the typical band width in the transition metals. In contrast to the work of Tsymbal et al. [39] the contributions to the conductivity arising from interband transitions are expected to be small.

SUMMARY

In conclusion, the self-consistent calculation of the scattering properties and the improved treatment of the Boltzmann transport equation including vertex corrections provide a powerful tool for a comprehensive theoretical description and a helpful insight into the microscopic processes of CIP-GMR. The experimentally found trends concerning the doping with various materials at different positions in the magnetic multilayer could be well reproduced which means that spin-dependent impurity scattering is the most important source of GMR. The theoretical results show furthermore that interface scattering caused by intermixing plays a crucial role and has to be taken into account in any system under consideration. Selective doping of the multilayer with impurities in specific positions causes variations of GMR which could be well understood by the modulation of spin-dependent scattering due to quantum confinement in the layered system and by the spin anisotropy.

Financial support by the DFG (FG 404) and BMBF contract 13N7379 is kindly acknowledged.

Electronic address: Zahn@physik.uni-halle.de

- ^y present address: Heyde AG, Auguste-Viktoria-Str. 2, D-61231 Bad Nauheim, Germany
- [1] M.N. Baibich, J.M. Broto, A. Fert, F. Nguyen Van Dau, F. Petroff, P. Etienne, G. Creuzet, A. Friederich, and J. Chazelas, Phys. Rev. Lett. **61**, 2472 (1988)
 - [2] G. Binasch, P. Grünberg, F. Saurenbach, and W. Zinn, Phys. Rev. B **39**, 4828 (1989).
 - [3] E. Tsymbal and D.G. Pettifor, Solid State Phys. **56**, 113 (2001).
 - [4] I. Mertig and P.M. Levy, *Theory of GMR in Spin dependent transport in magnetic nanostructures*, edited by S. Maekawa, Taylor & Francis, London (2002).
 - [5] S.S.P. Parkin, Phys. Rev. Lett. **71**, 1641 (1993).
 - [6] C.H. Marrows and B.J. Hickey, Phys. Rev. B **63**, 220405 (2001).
 - [7] P. M. Levy, Solid State Phys. **47**, 367 (1994).
 - [8] P. Zahn, J. Binder, I. Mertig, R. Zeller, and P.H. Dederichs, Phys. Rev. Lett. **80**, 4309 (1998).
 - [9] C. Blaas, P. Weinberger, L. Szunyogh, P.M. Levy, and C. Sommers, Phys. Rev. B **60**, 492 (1999).
 - [10] J. Unguris, R.J. Celotta, and D.T. Pierce, Phys. Rev. Lett. **79**, 2734 (1997).
 - [11] J. Opitz, P. Zahn, J. Binder, and I. Mertig, Phys. Rev. B **63**, 094418 (2001).
 - [12] R. Zeller, P.H. Dederichs, B. Újfalussy, L. Szunyogh, and P. Weinberger, Phys. Rev. B **52**, 8807 (1995).
 - [13] V.L. Moruzzi and P.M. Marcus, Phys. Rev. B **46**, 3171 (1992).
 - [14] R. Zeller and P.H. Dederichs, Phys. Rev. Lett. **42**, 1713 (1979).
 - [15] P.M. Oppeneer and A. Lodder, J. Phys. F **17**, 1885 (1987), *ibid* 1901 (1987).
 - [16] I. Mertig, Rep. Prog. Phys. **62**, 237 (1999).
 - [17] I. Mertig, E. Mrosan, and P. Ziesche, *Multiple Scattering Theory of Point Defects in Metals: Electronic Properties*, Teubner-Verlag, Leipzig (1987)
 - [18] P.M. Oppeneer and A. Lodder, J. Phys. F **17**, 1885 (1987).
 - [19] P.M. Oppeneer and A. Lodder, J. Phys. F **17**, 1901 (1987).
 - [20] J.C. Swihart, W.H. Butler, G.M. Stocks, D.M. Nicholson, and R.C. Ward, Phys. Rev. Lett. **57**, 1181 (1986).
 - [21] R.E. Camley and J. Barnaś, Phys. Rev. Lett. **63**, 664 (1989).
 - [22] R.Q. Hood, and L.M. Falicov, Phys. Rev. B **46**, 8287 (1992).
 - [23] P. Zahn, I. Mertig, M. Richter, and H. Eschrig, Phys. Rev. Lett. **75**, 2996 (1995).
 - [24] W.H. Butler, X.-G. Zhang, D.M.C. Nicholson, T.C. Schulthess, and J.M. MacLaren, Phys. Rev. Lett. **76**, 3216 (1996).
 - [25] X.-G. Zhang and W.H. Butler, J. Appl. Phys. **87**, 5176 (2000).
 - [26] N.C. Mott, Adv. Phys. **13**, 325 (1964)
 - [27] P. Zahn, N. Papanikolaou, F. Erler, and I. Mertig, Phys. Rev. B **65**, 134432 (2002).
 - [28] M.D. Stiles, J. Appl. Phys. **79**, 5805 (1996).
 - [29] D.T. Dekadjevi, P.A. Ryan, B.J. Hickey, B.D. Fulthorpe, and B.K. Tanner, Phys. Rev. Lett. **86**, 5787 (2001).
 - [30] D.J. Larson, A.K. Petford-Long, A. Cerezo, G.D.W. Smith, D.T. Foord, and T.C. Anthony, Appl. Phys. Lett. **73**, 1125 (1998).
 - [31] J. Schleiwies, G. Schmitz, S. Heitmann, and A. Hütten, Appl. Phys. Lett. **78**, 3439 (2001).
 - [32] A. Davies, J.A. Strosio, D.T. Pierce, and R.J. Celotta, Phys. Rev. Lett. **76**, 4175 (1996).
 - [33] R. Schad, P. Belien, G. Verbanck, K. Temst, V.V. Moshchalkov, Y. Bruynseraede, D. Bahr, J. Falta, J. Dekoster, and G. Langouche, Europhys. Lett. **44**, 379 (1998).
 - [34] M.C. Cyrille, S. Kim, M.E. Gomez, J. Santamaria, K.M. Krishnan, and I.K. Schuller, Phys. Rev. B **62**, 3361 (2000).
 - [35] P. Zahn et al., Phys. Rev. Lett. **80**, 4309 (1998).
 - [36] C.H. Marrows et al., Phys. Rev. B **63**, 220405 (2001).
 - [37] F. Erler, P. Zahn, and I. Mertig, Phys. Rev. B **64**, 094408 (2001).
 - [38] P. Zahn and I. Mertig, Phys. Rev. B **63**, 104412 (2001).
 - [39] E.Yu. Tsymbal and D.G. Pettifor, Phys. Rev. B **54**, 15314 (1996).